NASA-TM-72868 19790023980

NASA Technical Memorandum 72868

EFFECT OF ELEMENT DENSITY ON THE NASTRAN CALCULATED MECHANICAL AND THERMAL STRESSES OF A SPAR

Jerald M. Jenkins

October 1979

NASA

NASA Technical Memorandum 72868

EFFECT OF ELEMENT DENSITY ON THE NASTRAN CALCULATED MECHANICAL AND THERMAL STRESSES OF A SPAR

Jerald M. Jenkins
Dryden Flight Research Center
Edwards, California

National Aeronautics and
Space Administration

1979

EFFECT OF ELEMENT DENSITY ON THE NASTRAN CALCULATED MECHANICAL AND THERMAL STRESSES OF A SPAR

Jerald M. Jenkins
Dryden Flight Research Center

INTRODUCTION

Aircraft which accumulate significant flight time at speeds sufficient to produce severe aerodynamic heating (refs. 1 to 3) also produce thermal stresses which must be predicted. Some information has been reported (refs. 4 to 6) which identifies the structural model detail that is required to predict thermal stresses in a small built-up structure. This information indicates that a large number of elements are required to calculate an accurate answer. A large model quickly becomes a cost problem for the large structure application. This paper addresses the effect of changing the element density of the structural model on the mechanical and thermal stresses using NASA structural analysis (NASTRAN) (ref. 7). Changing the element density in certain areas of large structures may be the logical answer to avoiding exceptionally large models from both the structural and thermal viewpoints.

A spar is mathematically defined and modeled using NASTRAN. The element density along the length of the spar is changed and the resulting variations in stress distributions are studied. The effects of surface tractions and constraints are also examined to determine the effect on the stress distributions.

DESCRIPTION OF THE SPAR

The spar shown in figure 1 (top) consisting of upper and lower flanges connected by a web is the structure used for the analytical study. The spar is 1.83 meters (72 inches) long with a depth of .56 meters (22 inches) and a flange width of .30 meters (12 inches). Both the web thickness and the flange thickness is .05 meters (2 inches).

DESCRIPTION OF THE NASTRAN MODEL

The NASTRAN model of the spar is shown in figure 1 (bottom). The model consists of 112 elements of which 80 elements are bars and 32 elements are shear panels. The model was developed with 49 grid points and 238 degrees of freedom. There were 177 bulk data cards. The grid point numbers are presented in figure 1. As can be seen, the element density of the model decreases from eleven bars then to five bars and finally to three bars in the longitudinal direction. This decrease in element density (and its effect on the magnitude and distribution of stresses) is the primary study parameter of this report. All rotations and displacements were constrained at one end of the beam with the exception of the displacement through the depth of the spar.

DESCRIPTION OF THE LOADING

Two loading conditions were imposed on the NASTRAN model of the previously described spar. A force of 44482 newtons (10000 pounds) was applied to the end of the spar (see figure 2) while the other end was constrained like a cantilevered beam. The problem was also run with the constrained end and the loaded end reversed so that the effects of the constraint and the load location (surface traction) on the calculated stresses could be studied.

A temperature distribution ranging from 1367 degrees Kelvin (2000 degrees Fahrenheit) at the bottom cap of the spar to 256 degrees Kelvin (0 degrees Fahrenheit) at the top cap of the spar (see bottom of figure 2) was applied to the model of the spar to examine thermal stresses. The temperature distribution is arbitrary and is applied only to examine variations in calculated axial thermal stresses due to changes in element density.

RESULTS AND DISCUSSION

Thermal stresses and bending stresses in the axial direction

are presented in Tables I through IV. In Table I, thermal stresses are presented for the left end constraint (see figure 2) while thermal stress data for the right end constraint is presented in Table II. Bending stresses for the left end constrained with a right end loading are presented in Table III. Bending stresses for the right end constrained with a left end loading are presented in Table IV. A cross-correlation between the model element number listed in the tables and the connecting grid points is presented in Table V.

The tables are arranged such that the depth of the spar can be studied from top to bottom in the tables. The spar length variations can be observed by left to right examination of the tables. The first two stress columns represent the high element density areas (elements 1 through 22). The third and fourth stress columns represent the intermediate element density areas (elements 23 through 32). The fifth and sixth stress columns represent the low element density areas (elements 33 through 38). The high element density area has eleven elements, the intermediate element density area has five elements, and the low element density area has three elements across the depth of the model of the spar.

Temperature Loading

The thermal stress calculated using the NASTRAN model of the spar is plotted at various spar depths in figure 3. The thermal stresses result from the temperature distribution shown in figure 2. It can be seen by comparing the data at section A-A with the data at section B-B that only minor variations result near the constrained end. The variations in element density do, however, relult in large variations of axial thermal stress through the spar depth. It can be seen that very large tensile thermal stresses occur at the eleven element density (sections A-A and B-B) near the .3 meter (12 inch) depth. However, for the five element density (sections C-C and D-D) and the three element density (sections E-E and F-F) areas, the axial thermal stress is only a fraction of the stresses at the eleven element density areas. Significant variations among the distributions at the eleven, five, and three element areas occur throughout the depth of the spar.

Tables I and II compare thermal stresses calculated for the same temperature distribution but for opposite ends constrained. It can be easily seen that significant variations occur between Table I and Table II near the ends. Therefore, it must be noted that the constraint does affect the calculated thermal stresses as does the element density.

Mechanical Loading

The bending stresses resulting from the concentrated load at the end of the cantilevered spar are presented in Tables III and IV. The stresses are plotted for the left end constraint case in figure

4. Examination of the data in Tables III and IV reveals that the element density has little effect on the resulting calculated bending stresses. It can be concluded that the element density variations studied herein have no effect on the calculated bending stresses of an end-loaded cantilevered spar.

CONCLUDING REMARKS

A NASTRAN model of a spar was examined to determine the sensitivity of calculated axial thermal stresses and bending stresses to changes in element density of the model. The thermal stresses calculated with three different element densities resulted in drastically differing values. The position of the constraint also significantly affected the value of the calculated thermal stresses. Mechanical stresses calculated from an applied loading were insensitive to element density.

Dryden Flight Research Center
National Aeronautics and Space Administration
Edwards, Calif., September 7, 1979

REFERENCES

1. Quinn, Robert D.; and Olinger, Frank V. (appendix A by James C. Dunavant and Robert L. Stallings, Jr.): Heat-Transfer Measurements Obtained on the X-15 Airplane Including Correlations With Wind Tunnel Results. NASA TM X-1705, 1969.

2. Andrews, William H.: Summary of Preliminary Data Derived From the XB-70 Airplanes. NASA TM X-1240, 1966.

3. Quinn, Robert D.; and Olinger, Frank V.: Flight Temperatures and Thermal Simulation Requirements. NASA YF-12 Flight Loads Program. NASA TM X-3061, 1974 pp. 145-183.

4. Jenkins, Jerald M.; Schuster, Lawrence S.; and Carter, Alan L.: Correlation of Predicted and Measured Thermal Stresses on a Truss-type Aircraft Structure. NASA TM-72857, November, 1978.

5. Jenkins, Jerald M.: Correlation of Predicted and Measured Thermal Stresses On An Advanced Aircraft Structure With Similar Materials. NASA TM-72862, April 1979.

6. Jenkins, Jerald M.: Correlation of Predicted and Measured Thermal Stresses On An Advanced Aircraft Structure With Dissimilar Materials. NASA TM-72865, June 1979.

7. McCormick, Caleb W.,ed.: The NASTRAN User's Manual (Level 15). NASA SP-222(01), 1972.

TABLE I. - THERMAL STRESSES WITH LEFT END CONSTRAINT

Element Number	Stress, MN/m^2 (Kpsi)	Element Number	Stress, MN/m^2 (Kpsi)	Element Number	Stress, MN/m^2 (Kpsi)	Element Number	Stress, MN/m^2 (Kpsi)	Element Number	Stress, MN/m^2 (Kpsi)	Element Number	Stress, MN/m^2 (Kpsi)
1	-165(-24)	12	-200(-29)	23	-179(-26)	28	-179(-26)	33	0(0)	36	34(0)
2	62(9)	13	76(11)								
3	303(44)	14	351(51)	24	386(56)	29	345(50)				
4	551(80)	15	627(91)								
5	827(120)	16	910(132)								
6	255(37)	17	331(48)	25	358(52)	30	393(57)	34	235(34)	37	255(37)
7	-234(-34)	18	-179(-26)								
8	-324(-47)	19	-289(-42)								
9	-275(-40)	20	-269(-39)	26	-276(-40)	31	-206(-30)				
10	-172(-25)	21	-179(-26)								
11	0(0)	22	-27(-4)	27	-55(-8)	32	-82(-12)	35	-351(-51)	38	-420(-61)

TABLE II. - THERMAL STRESSES WITH RIGHT END CONSTRAINT

Element Number	Stress, MN/m^2 (Kpsi)	Element Number	Stress, MN/m^2 (Kpsi)	Element Number	Stress, MN/m^2 (Kpsi)	Element Number	Stress, MN/m^2 (Kpsi)	Element Number	Stress, MN/m^2 (Kpsi)	Element Number	Stress, MN/m^2 (Kpsi)
1	-206(-30)	12	-206(-30)	23	-179(-26)	28	-179(-26)	33	14(2)	36	55(8)
2	76(11)	13	76(11)								
3	358(52)	14	351(51)	24	386(56)	29	338(49)				
4	641(93)	15	634(92)								
5	924(134)	16	917(133)								
6	345(50)	17	345(50)	25	358(52)	30	386(56)	34	214(31)	37	165(24)
7	-165(-24)	18	-165(-24)								
8	-283(-41)	19	-282(-41)								
9	-269(-39)	20	-268(-39)	26	-276(-40)	31	-214(-31)				
10	-179(-26)	21	-179(-26)								
11	-34(-5)	22	-27(-4)	27	-55(-8)	32	-82(-12)	35	-330(-48)	38	-296(-43)

TABLE III. - BENDING STRESSES WITH LEFT END CONSTRAINT

Element Number	Stress, MN/m^2 (Kpsi)	Element Number	Stress, MN/m^2 (Kpsi)	Element Number	Stress, MN/m^2 (Kpsi)	Element Number	Stress, MN/m^2 (Kpsi)	Element Number	Stress, MN/m^2 (Kpsi)	Element Number	Stress, MN/m^2 (Kpsi)
1	-7.69(-1.15)	12	-6.41(-0.93)	23	-5.03(-0.73)	28	-3.45(-0.50)	33	-2.21(-0.32)	36	-0.83(-0.12)
2	-6.21(-0.90)	13	-5.17(-0.75)								
3	-4.62(-0.67)	14	-3.93(-0.57)	24	-2.96(-0.43)	29	-2.28(-0.33)				
4	-3.03(-0.44)	15	-2.69(-0.39)								
5	-1.45(-0.21)	16	-1.38(-0.20)								
6	0.07(0.01)	17	-0.07(-0.01)	25	0.00(0.00)	30	0.00(0.00)	34	0.07(0.01)	37	0.07(0.01)
7	1.59(0.23)	18	1.24(0.18)								
8	3.17(0.46)	19	2.55(0.37)								
9	4.69(0.68)	20	3.86(0.56)	26	2.96(0.43)	31	2.28(0.33)				
10	6.21(0.90)	21	5.17(0.75)								
11	7.86(1.14)	22	6.48(0.94)	27	5.03(0.73)	32	3.45(0.50)	35	2.14(0.31)	38	0.76(0.11)

TABLE IV. - BENDING STRESSES WITH RIGHT END CONSTRAINT

Element Number	Stress, MN/m^2 (Kpsi)	Element Number	Stress, MN/m^2 (Kpsi)	Element Number	Stress, MN/m^2 (Kpsi)	Element Number	Stress, MN/m^2 (Kpsi)	Element Number	Stress, MN/m^2 (Kpsi)	Element Number	Stress, MN/m^2 (Kpsi)
1	-0.69(-0.10)	12	-2.07(-0.30)	23	-3.59(-0.52)	28	-5.03(-0.73)	33	-6.62(-0.96)	36	-7.72(-1.12)
2	-0.59(-0.09)	13	-1.72(-0.25)								
3	-0.41(-0.06)	14	-1.24(-0.18)	24	-2.07(-0.30)	29	-2.96(-0.43)				
4	-0.28(-0.04)	15	-0.76(-0.11)								
5	-0.12(-0.02)	16	-0.35(-0.05)								
6	0.00(0.00)	17	0.07(0.01)	25	0.00(0.00)	30	0.00(0.00)	34	0.00(0.00)	37	0.07(0.01)
7	0.17(0.02)	18	0.48(0.07)								
8	0.35(0.05)	19	0.90(0.13)								
9	0.48(0.07)	20	1.31(0.19)	26	2.14(0.31)	31	2.96(0.43)				
10	0.59(0.09)	21	1.72(0.25)								
11	0.69(0.10)	22	2.14(0.31)	27	3.59(0.52)	32	5.03(0.73)	35	6.62(0.96)	38	7.65(1.11)

TABLE V. - IDENTIFICATION OF ELEMENTS WITH CONNECTING GRID POINTS

Element Number	Connecting Grid Points
1	1 - 12
2	2 - 13
3	3 - 14
4	4 - 15
5	5 - 16
6	6 - 17
7	7 - 18
8	8 - 19
9	9 - 20
10	10 - 21
11	11 - 22
12	12 - 23
13	13 - 24
14	14 - 25
15	15 - 26
16	16 - 27
17	17 - 28
18	18 - 29
19	19 - 30
20	20 - 31
21	21 - 32
22	22 - 33
23	23 - 34
24	25 - 35
25	28 - 36
26	31 - 37
27	33 - 38
28	34 - 39
29	35 - 40
30	36 - 41
31	37 - 42
32	38 - 43
33	39 - 44
34	41 - 45
35	43 - 46
36	44 - 47
37	45 - 48
38	46 - 49

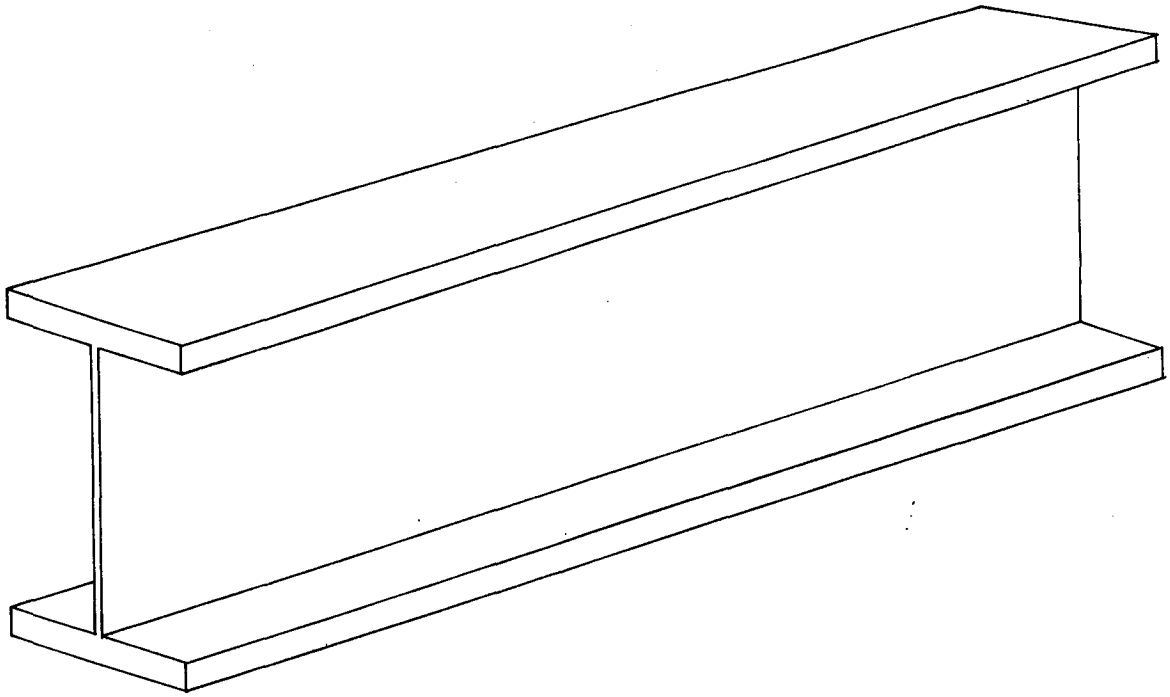

SPAR USED FOR ANALYSIS

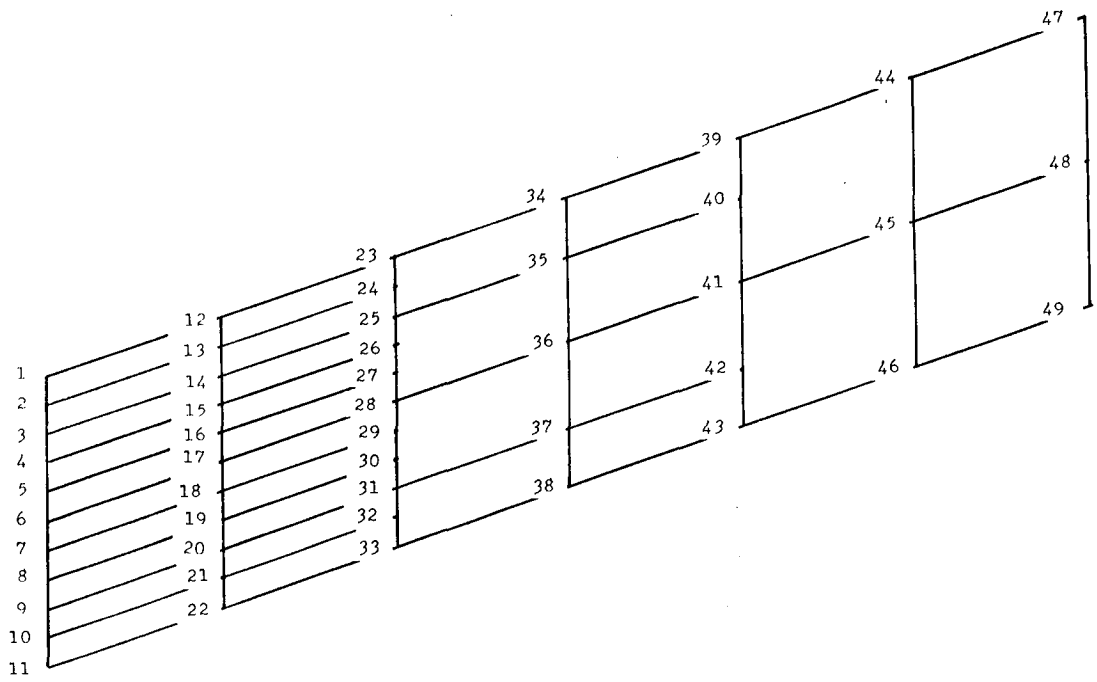

NASTRAN MODEL OF SPAR

Figure 1. Sketch of spar used for analysis and NASTRAN representation.

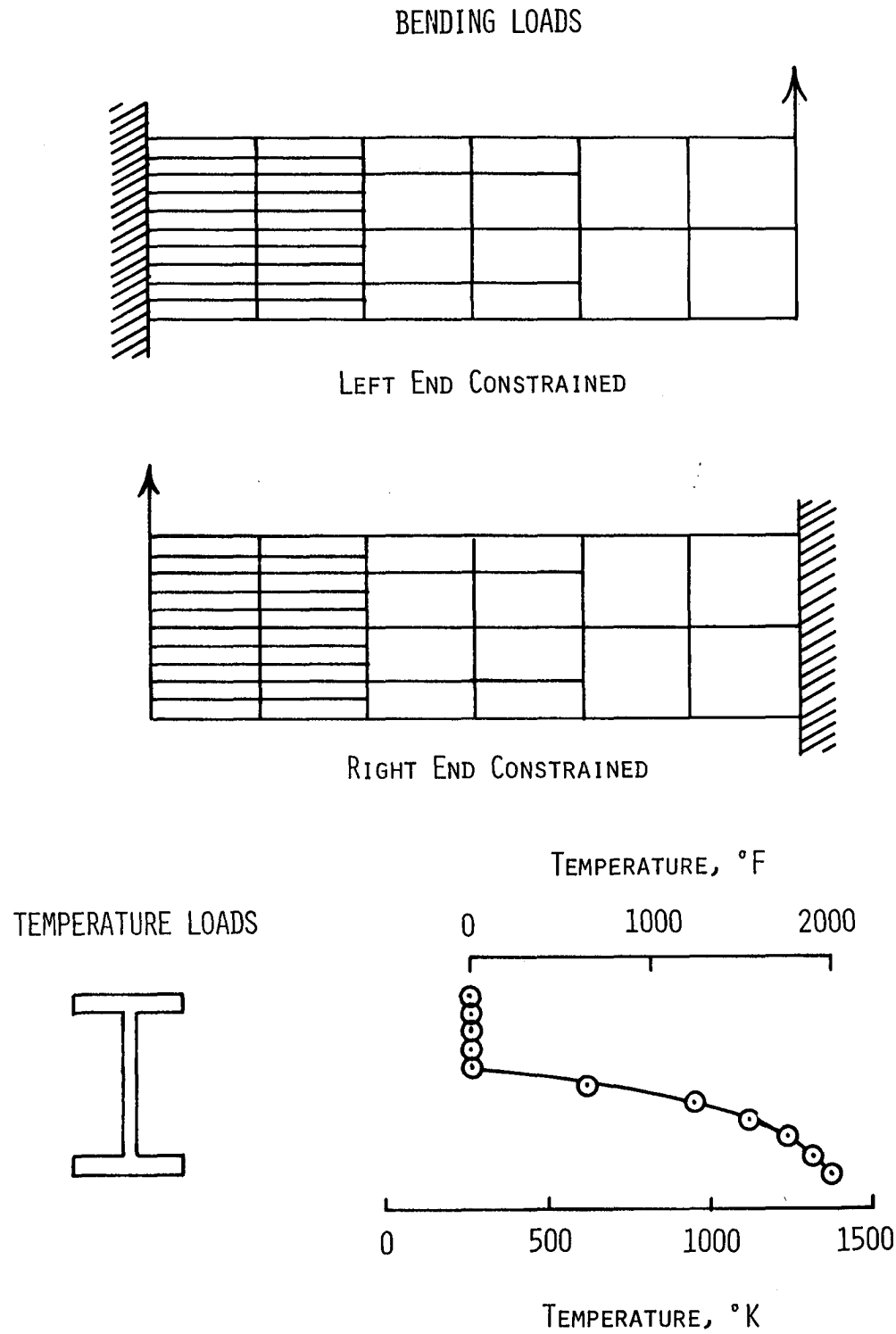

Figure 2. Mechanical and thermal spar loadings including constraint conditions.

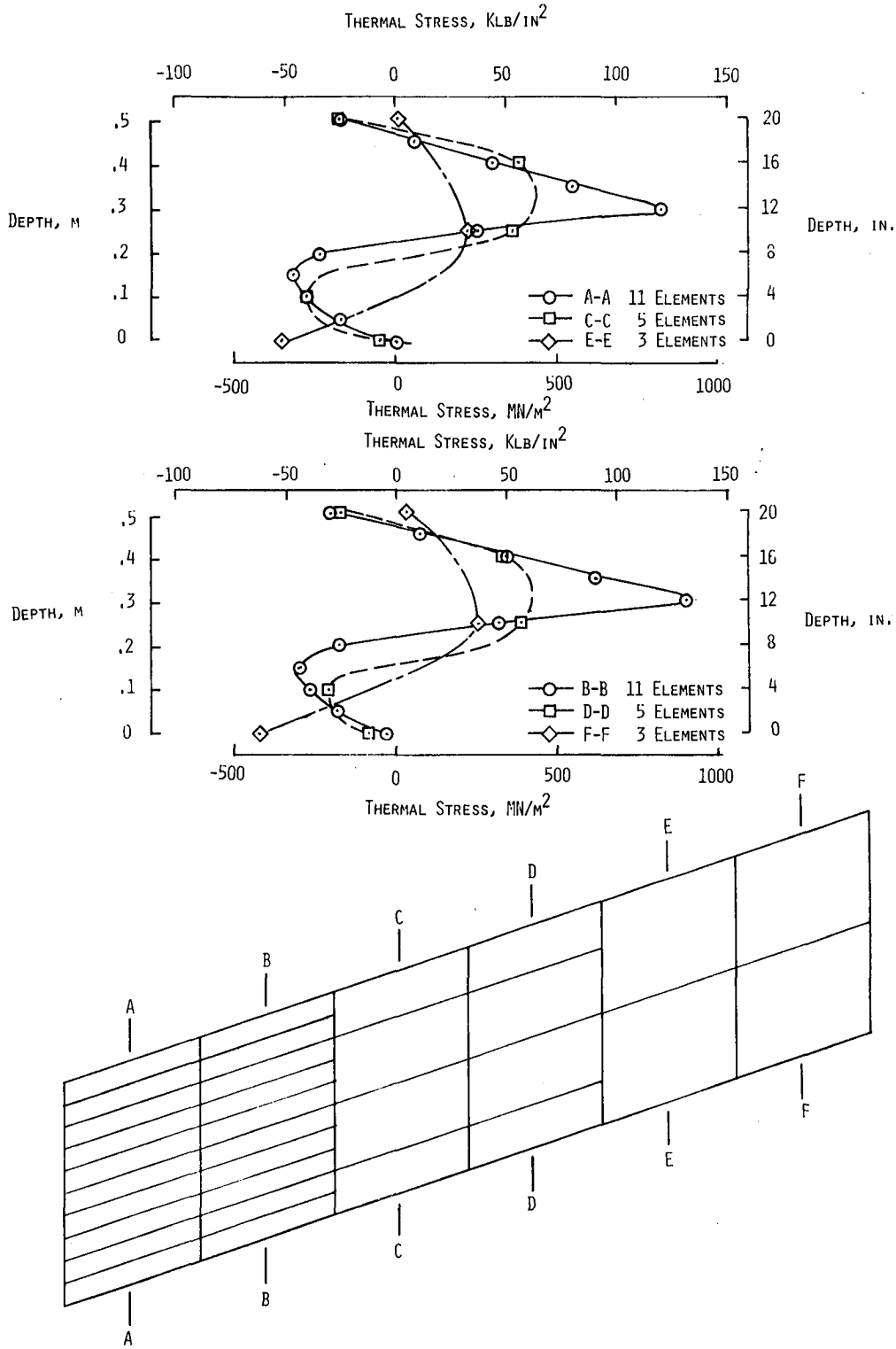

Figure 3. Variation of axial thermal stress with spar depth for varying element density.

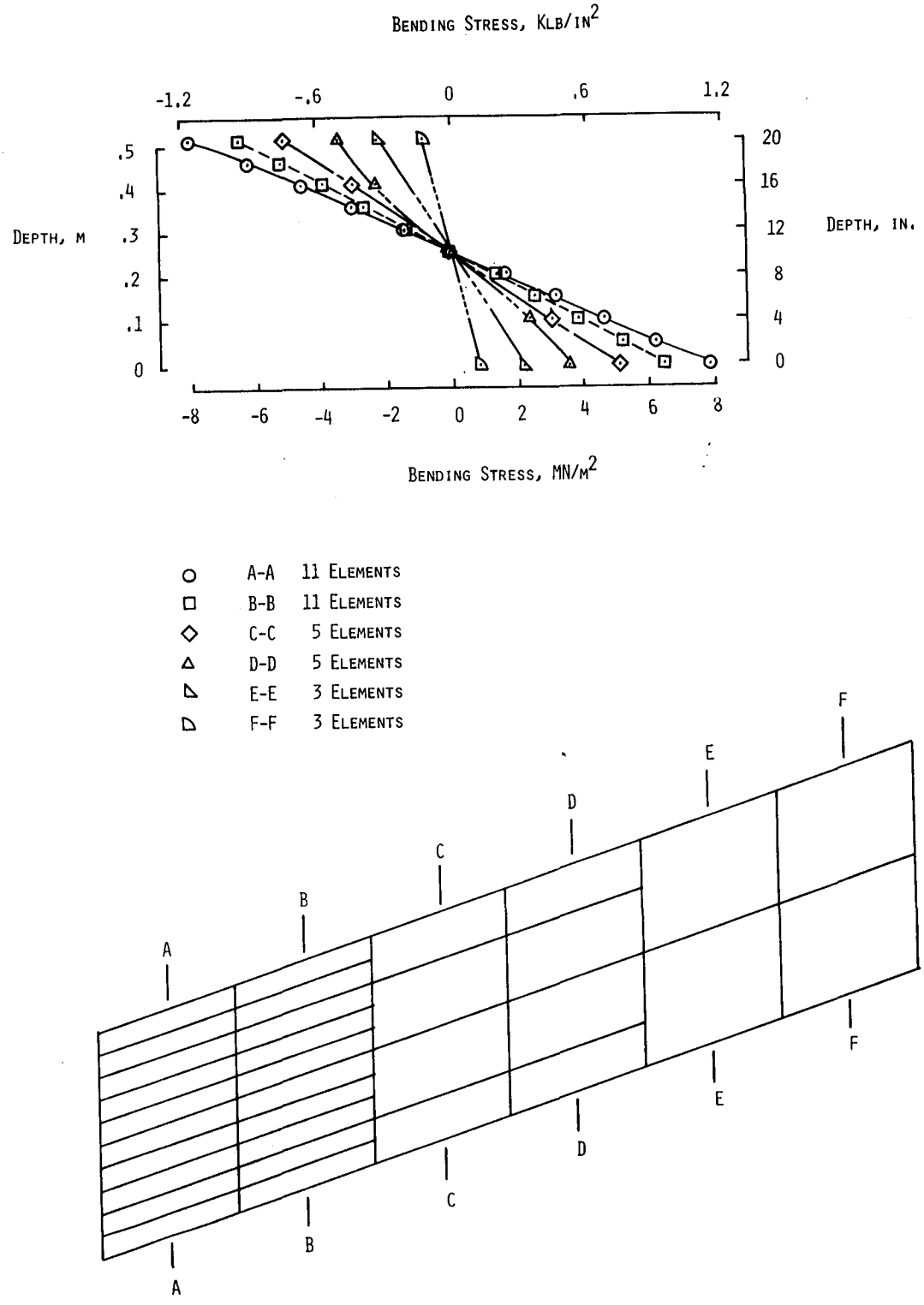

Figure 4. Variation of bending stress with spar depth for varying element density.

1. Report No.	2. Government Accession No.	3. Recipient's Catalog No.
NASA TM-72868		

4. Title and Subtitle	5. Report Date
EFFECT OF ELEMENT DENSITY ON THE NASTRAN CALCULATED MECHANICAL AND THERMAL STRESSES OF A SPAR	October 1979
	6. Performing Organization Code
7. Author(s)	8. Performing Organization Report No.
Jerald M. Jenkins	H-1104
	10. Work Unit No.
9. Performing Organization Name and Address	505-02-54
NASA Dryden Flight Research Center P. O. Box 273 Edwards, California 93523	11. Contract or Grant No.
	13. Type of Report and Period Covered
12. Sponsoring Agency Name and Address	Technical Memorandum
National Aeronautics and Space Administration Washington, D.C. 20546	14. Sponsoring Agency Code

15. Supplementary Notes

16. Abstract

A NASTRAN model of a spar was examined to determine the sensitivity of calculated axial thermal stresses and bending stresses to changes in element density of the model. The thermal stresses calculated with three different element densities resulted in drastically differing values. The position of the constraint also significantly affected the value of the calculated thermal stresses. Mechanical stresses calculated from an applied loading were insensitive to element density.

17. Key Words (Suggested by Author(s))	18. Distribution Statement
Thermal stresses Finite element models Structural modeling	Unclassified—Unlimited STAR category: 01

19. Security Classif. (of this report)	20. Security Classif. (of this page)	21. No. of Pages	22. Price*
Unclassified	Unclassified	15	$3.25

For sale by the National Technical Information Service, Springfield, Virginia 22161